Electronic reconstruction of hexagonal FeS: a view from density functional dynamical mean-field theory

2017 Mater. Res. Express 4 036303

(http://iopscience.iop.org/2053-1591/4/3/036303)

Materials Research Express

OPEN ACCESS

RECEIVED
19 October 2016

REVISED
8 February 2017

ACCEPTED FOR PUBLICATION
23 February 2017

PUBLISHED
16 March 2017

PAPER

Electronic reconstruction of hexagonal FeS: a view from density functional dynamical mean-field theory

L Craco[1,3], J L B Faria[1] and S Leoni[2]

[1] Instituto de Física, Universidade Federal de Mato Grosso, 78060-900, Cuiabá, MT, Brazil
[2] School of Chemistry, Cardiff University, Cardiff, CF10 3AT, United Kingdom
[3] Author to whom any correspondence should be addressed.

E-mail: lcraco@fisica.ufmt.br

Keywords: LDA+DMFT, electronic structure, metal-insulator transitions, many-electron systems

Abstract

We present a detailed study of correlation- and pressure-induced electronic reconstruction in hexagonal iron monosulfide, a system which is widely found in meteorites and one of the components of Earth's core. Based on a perusal of experimental data, we stress the importance of multi-orbital electron-electron interactions in concert with first-principles band structure calculations for a consistent understanding of its intrinsic Mott–Hubbard insulating state. We explain the anomalous nature of pressure-induced insulator-metal-insulator transition seen in experiment, showing that it is driven by dynamical spectral weight transfer in response to changes in the crystal-field splittings under pressure. As a byproduct of this analysis, we confirm that the electronic transitions observed in pristine FeS at moderated pressures are triggered by changes in the spin state which causes orbital-selective Kondo quasiparticle electronic reconstruction at low energies.

1. Introduction

Stoichiometric FeS is known to be a natural occurring mineral and has been investigated in fields as diverse as space science [1–3], geosciences [4], crystal chemistry [5] and condensed matter physics [6–9], because it is a possible core material for the terrestrial planets and one of the fundamental components of meteorites. Hence, similar to the classical Mott–Hubbard insulator FeO [10, 11], FeS is considered to be an important material for solid state and earth sciences. Apart from this, hexagonal iron monosulfide has also been investigated in field as diverse as applied surface sciences [12] or as potential material for future energy storage and lithium-ion battery applications [13].

As revealed by high-pressure x-ray diffraction measurements [1, 3, 5, 14], FeS undergoes a series of structural phase transitions with increasing pressure (P): a detailed description of the $P \times T$ structural phase transformations of FeS can be found, for example, in [2] and [5]. From these studies it is known that under ambient conditions troilite FeS has a hexagonal structure (space group $P-62c$) which is derivative of the NiAs unit cell with axis lengths $a = \sqrt{3}\,c_f = 5.955$ Å and $2c_f = 11.76$ Å [14], where c_f is the lattice parameter of the fundamental NiAs subcell. The corresponding crystal structure of troilite FeS is shown in figure 1, see also [14]. As seen in this figure, increasing pressure at room temperature results in a structural phase transition close to 3.5 GPa to an hexagonal NiAs-type structure (here dubbed as h-FeS) [2] with space group $P\ 63/mmc$. With further increasing P at temperatures close to room-T results in an additional structural transformation at around 7 GPa to a monoclinic unit cell (space group $P2_1$ or $P2_1/m$) [14]. It is worth noting as well that the change of the sulfur sublattice might transform the layered structure of tetragonal FeS (mackinawite) to the three-dimensional NiAs-type structure of hexagonal pyrrhotite [15]. Thus, it is clear that FeS adopts a variety of crystallographic structures under different sample preparations [15, 16] or $P \times T$ conditions [2].

Interestingly, iron monosulfides, such as troilite [14, 17, 18] and mackinawite [16, 19–22], show a variety of structural, magnetic and transport properties which are not fully understood yet. At ambient pressure (AP), troilite is an antiferromagnetic insulator with a Néel transition temperature of 589 K [18]. Similar to tetragonal iron-chalcogenide superconductors [23]. FeS is a correlated electron system where the on-site Coulomb

repulsion U is sizable [6], i.e. of the order of the one-particle bandwidth W. At room-T and AP conditions troilite is insulating and has an energy gap of $\approx$ 0.1 eV [24] and a high resistivity value of $\approx$ 5.2 10^{-2} Ωcm [25]. As clearly indicated by resistivity measurements, FeS undergoes to successive electronic transitions with increasing pressure at room temperature. Below 2.8 GPa the electrical resistivity[$\rho(T)$]of FeS decreases exponentially with increasing temperature [18] and pressure [25], and abruptly decreases around 3.5 GPa. Interestingly, $\rho(T)$ decreases at pressures up to 6.6 GPa and then starts to increase with increasing external pressure [14, 25]. This anomalous pressure dependence can be taken as an evidence of unconventional electronic reconstruction which might be linked to the onset of structural transition from hexagonal to monoclinic phases [5, 14]. It should be noted that the nature of electrical transport and magnetism of FeS at high pressures have been rationalized in terms of pressure-induced high-spin (HS) to low-spin (LS) state transition [7, 14]. This scenario was based on a combined study ^{57}Fe Mössbauer and resistivity data [14] as well as on high-pressure synchrotron x-ray emission spectroscopy measurements [7]. In combination with magnetic susceptibility data [26]. these measurements have been taken as experimental evidences of the HS-to-LS state transition, where hexagonal FeS (h-FeS) has thermally activated charge carries within the $S = 2$ HS configuration while monoclinic FeS is considered to be in a LS ($S = 0$) state, characterized by quenched local moments [7, 14].

Based on careful perusal of experimental studies it is evident that h-FeS is an ideal system to explore pressure-induced electronic phase transitions of correlated electron systems [27]. We recall that the localized nature of troilite and its correlated electronic structure has been investigated by photoemission (PES) and inverse-photoemission spectroscopy experiments [6]. Based on this study it is known, for example, that the Fe 3d bandwidth in the PES spectra is 25–30% narrower than that predicted by first-principles band-structure calculations. The one-particle density-of-states (DOS) was shown to be accompanied by an intense tail at high binding energies, consistent with the correlated fingerprints found in 11 iron-chalcogenide superconductors [28]. Cluster-model calculations in [6] indicate Hubbard-like satellite structures at high energies for realistic values of the on-site Coulomb interaction between 4.0–5.0 eV, which have been confirmed by recent local-density-approximation plus dynamical-mean-field-theory (LDA+DMFT) calculations [36]. However, in spite of these studies the correlated electronic nature of h-FeS has not been explored so far. In this work we shed light onto this problem.

Density functional calculations for tetragonal FeS [29] demonstrate that the sulfer 3p states lie well below the Fermi level (E_F) and are weakly hybridized with Fe 3d states. Hence, as in tetragonal FeSe superconductor [31], the most relevant electronic states near E_F derive from Fe^{2+} (d^6 electronic configuration) with almost direct Fe–Fe hopping. In a previous work two of us undertook a comparative LDA+DMFT study [30] of hexagonal and tetragonal iron-selenide (FeSe) superconductor [31], showing the orbital-selective nature of the Mott–Hubbard insulating state in h-FeSe. This together with good semiquantitative agreement with extant experimental data (photoemission and inverse-photoemission spectroscopy) for troilite [36] serves as support to explore dynamical correlation effects and electronic reconstructions in h-FeS. A proper microscopic description of pressure-induced localization-delocalization transition [18, 25] and weak localization at higher pressures [14, 25] across the hexagonal-to-monoclinic phase boundary is important for understanding the role played by dynamical correlations in the low- and high-energy electronic states of iron-based materials and their possible implications for the internal structure of planetary cores and in the Earth's lower mantle [10, 11]. In this work we address the problem of multi-orbital (MO) electron-electron interactions in h-FeS, revealing the emergence of a correlation induced Mott–Hubbard insulating state with a band gap consistent with optical data [24]. We also provide a compreensive theoretical description of MO electronic reconstruction in FeS, showing resistivity results which are in good qualitative agreement with extant transport experiments at moderated pressures [14, 25].

2. Results and discussion

2.1. Electronic structure of hexagonal FeS

Within the hexagonal (NiAs-type) structure [14], see figure 1, one-electron band structure calculations based on LDA were performed for the h-FeS system using the linear muffin-tin orbitals (LMTO) scheme [32], in the atomic sphere approximation: This approximation provides reliable results at one-particle level and has been used to study the electronic structure of different materials [33], including iron, sulfur, and oxygen at high pressures [34] and iron sulfides [35]. Here, self-consistency is reached by performing calculations with 549 irreducible $\mathbf{k}$-points. The radii of the atomic spheres were chosen as $r = 2.78$ (Fe) and $r = 2.74$ (S) a.u. in order to minimize their overlap.

To elucidate the differences between the bare electronic structure of troilite FeS [36] as well as hexagonal and monoclinic [37][4] FeS in figure 2 we display their total LDA DOS. As seen, for the lower pressure structural phases the one-particle bandwidth corresponding to Fe-3d states is close to 4.2 eV, a result which is in good agreement with recent GGA calculations for troilite FeS at ambient pressures [9]. Also consistent with this correlated, *ab initio* study on pressurized FeS, we observe a satellite structure centered around 3.9 eV binding energy which arrises from the hybridization between Fe-3d and S 3p states. As expected, this overlap is enhanced due to a more com-

[4] The crystal structure data for monoclinic FeS used in our LDA calculation is found, for example, at Nelmes *et al* [37].

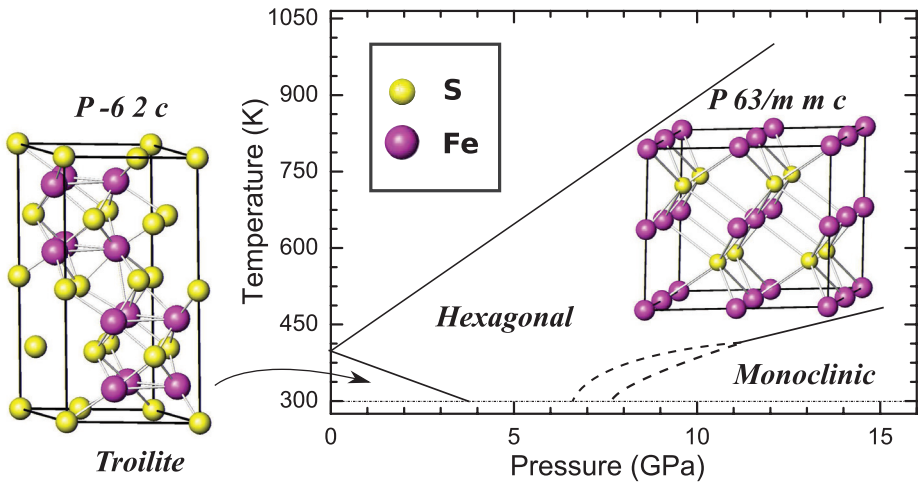

Figure 1. Structural phase diagram of pressurized FeS. As in [14] the dashed lines between 6.5–7.5 GPa demarcate the pressure range where the hexagonal and monoclinic phases coexist. In the two crystal structure of FeS, the large and small spheres represent Fe and S atoms, respectively. To illustrate the relative arrangement of atoms, the origin of the unit cell is chosen at Fe positions.

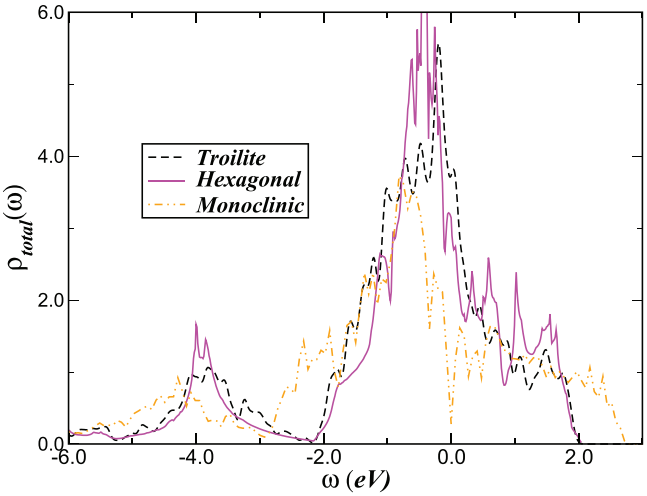

Figure 2. Total LDA density-of-states (DOS) for the Fe d-band of troilite (dashed lines), hexagonal (solid lines) and monoclinic (dot-dashed lines) FeS. Compared to troilite an important feature to be seen is the transfer of spectral weight and the depletion of one-band electronic states near E_F in h-FeS. Also interesting is the band-broadening (close to 1.5 eV) in monoclinic FeS compared the lower pressure phases.

pact hexagonal structure compared to troilite, see figure 1. Interestingly as well is the fact that we do not observe pronounced changes in the one-particle bandwidth between these two structural phases in the LDA results. Meaning, as assumed below, that the transfer of spectral spectral weight and the changes in the orbital-dependent on-site energy levels due to crystal-field effects and their interplay with sizable electron-electron interactions are intrinsic driving forces towards a reconstructed electronic state in pressurized h-FeS. Moreover, also in good accord with results of [9] is the appreciable band-broadening of 1.5 eV (induced by increased hopping amplitudes) seen in the electronic structure of monoclinic FeS. Albeit not shown, important changes in the orbital-selective band structure are expected to occur across the hexagonal-to-monoclinic structural phase transition in FeS but this comparative study is out of the scope of this work and it is left for future investigations. Finally, to illustrate the contribution from different 3d bands in figure 3 we display the orbital resolved LDA DOS of h-FeS. Thus, taken together our results in figures 2 and 3 with previous calculations for h-FeSe [31] as well as for FeS [9, 36] we confirm that the active electronic states in h-FeS involve the Fe 3d carriers, where all d-bands have appreciable weight at E_F. From LDA, the one-electron part of h-FeS is

$$H_0 = \sum_{\mathbf{k},a,\sigma} \epsilon_a(\mathbf{k}) c^{\dagger}_{\mathbf{k},a,\sigma} c_{\mathbf{k},a,\sigma} + \sum_{i,a,\sigma} \epsilon^{(0)}_a n_{i,a,\sigma}, \quad (1)$$

where $a = (x^2 - y^2, 3z^2 - r^2, xz, yz, xy)$ denote the diagonalized 3d orbitals of FeS. $\epsilon_a(\mathbf{k})$ is the one-electron band dispersion, which encodes details of the one-electron (LDA) band structure, and the $\epsilon^{(0)}_a$ are on-site orbital energies of h-FeS whose bare values are read off from LDA spectral functions. These are relevant one-particle

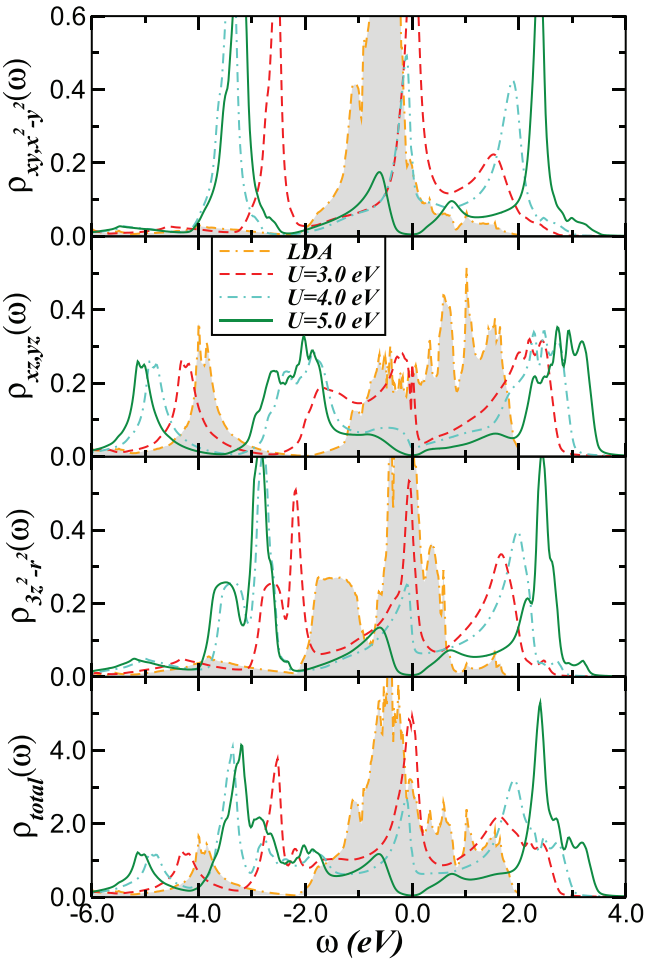

Figure 3. Orbital-resolved LDA and LDA+DMFT density-of-states (DOS) for the Fe d-orbitals of hexagonal FeS. An important feature to be seen in the fact that all d-bands in LDA span over the Fermi level, $E_F = \omega = 0$. This confirms that the electronic states relevant to hexagonal FeS are Fe 3d-states. Noteworthy are the electronic reconstruction with increasing on-site Coulomb interaction and the Mott–Hubbard insulating state with totally splitted LDA bands at E_F for $U = 5$ eV.

inputs for MO-DMFT which generates a Mott–Hubbard insulating state for $U = 5.0$ eV as shown below. The correlated many-body Hamiltonian for h-FeS reads

$$H_{\rm int} = U\sum_{i,a} n_{i,a,\uparrow}n_{i,a,\downarrow} + U' \sum_{i,a\neq b} n_{i,a}n_{i,b} - J_H \sum_{i,a\neq b} \mathbf{S}_{i,a}\cdot\mathbf{S}_{i,b}\,, \tag{2}$$

where U is the on-site Coulomb interaction [6], $U' = U - 2J_H$ is the inter-orbital Coulomb interaction term, and J_H is the Hund's coupling. We evaluate the many-particle Green's functions $[G_{a,\sigma}(\mathbf{k},\omega)]$ of the MO Hamiltonian $H = H_0 + H_{\rm int}$ within LDA+DMFT [30], using MO iterated perturbation theory (MO-IPT) as impurity solver [38]. The DMFT solution involves replacing the lattice model by a self-consistently embedded MO-Anderson impurity model, and the self-consistency condition requiring the local impurity Green's function to be equal to the local Green's function for the lattice. The full set of equations for the MO case can be found in [38], so we do not repeat the equations here. It worth mentioning, however, that the IPT is an interpolative *ansatz* that connects the two exactly soluble limits of the one-band Hubbard model [39], namely, the uncorrelated ($U = 0$) and the atomic ($\epsilon_{\mathbf{k}} = 0$) limits. It accounts for the correct low- and high-energy behavior of the one-particle spectra, and the correlated Fermi liquid (FL) behavior in the large-D limit (DMFT) [40]. It ensures the Mott–Hubbard metal-insulator transitions from a correlated FL metal to a Mott–Hubbard insulator as a function of the Coulomb interaction U. The IPT is known to be computationally vey efficient, with real frequency output at zero and finite temperatures. As shown below, the LDA+DMFT(MO-IPT) solution for h-FeS introduces non-trivial effects stemming from the dynamical nature of sizable electronic correlations. Namely, these processes lead to large transfer of spectral weight (SWT) across large energy scales in response to small changes in the electronic parameters, a characteristic lying at the heart of the anomalous responses of correlated electron systems.

Let us now discuss our LDA+DMFT results obtained within the d^6 electronic configuration of the Fe^{2+} in FeS. In figure 3 we display the effect of electron-electron interactions on the orbital-resolved and total spectral function of h-FeS. Similar to FeO [41], at $U = 5.0$ eV (and $J_H = 0.7$ eV) h-FeS is a MO Mott–Hubbard insulator with an orbital dependent band gap. Lower- (LHB) and upper- (UHB) Hubbard bands are visible, albeit to a

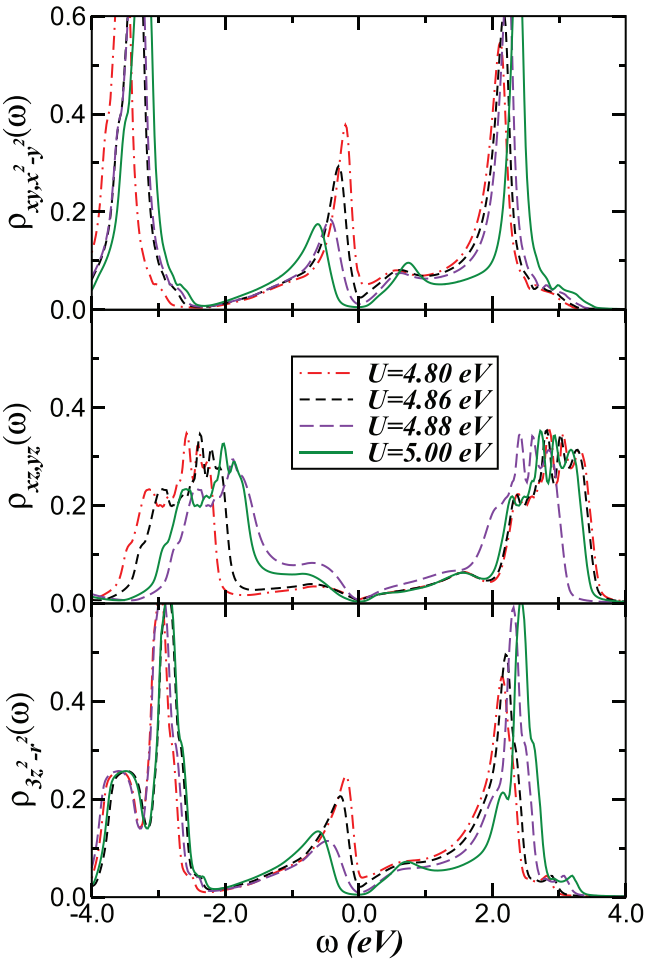

Figure 4. Orbital-resolved LDA+DMFT DOS for the Fe *d*-orbitals of hexagonal FeS across the correlation-induced metal-insulator transition. Large dynamical spectral weight transfer along with Mott–Hubbard localization is visible in the LDA+DMFT spectral functions.

different extent in all orbital-resolved spectral functions. As seen, the $xy, x^2-y^2, 3r^2-z^2$ orbitals show stronger correlation effects with pronounced Hubbard bands, while the *xz*,*yz* orbitals have less tendency towards local moment formation (LHB). Changes in the LDA+DMFT electronic structure are also observed throughout the total spectral function, showing large-scale changes in SWT with increasing *U*. As seen, in figure 3, the LDA+DMFT spectral functions are highly reshaped by electron-electron interactions compared to LDA, and future PES and x-ray absorption (XAS) experiments could verify this aspect.

For a more detailed analysis of dynamical MO electronic interaction effects in *h*-FeS, the orbital-resolved spectral functions across the correlation induced metal-insulator transition are shown in figure 4. Electronic correlations lead to interesting modifications of the correlated spectra. Below the critical value of Mott–Hubbard insulating phase ($U_c = 4.87$ eV) the many-body spectra describe an incoherent, non-Fermi liquid system with orbital dependent low-energy pseudogap features. Noteworthy is the suppression of the one-electron dispersion at low binding energies within the xy, x^2-y^2 orbitals with increasing *U*. (As shown below, these shoulder features are the precursors of coherent Kondo clouds in pressurized FeS.) Moreover, in both insulating and metallic phases, the double degenerated *xz*,*yz*-orbitals are Mott localized while the $xy, x^2-y^2, 3z^2-r^2$-orbitals are metallic below U_c. As seen, the LDA+DMFT electronic structure in figure 4 show large-scale changes in SWT at the critical phase boundary, 4.86 eV $< U_c <$ 4.88 eV, with concomitant suppression of hole- and electron-like bands at low energies in the Mott–Hubbard insulting phase.

2.2. Electronic reconstruction of pressurized FeS

We turn now to the effect of increasing pressure on the correlated electronic states of *h*-FeS system. Motivated by experimental evidences of spin-state (HS-to-LS) and structural (hexagonal-to-monoclinic) transitions in FeS under external pressure [14] we adopt the following strategy to study these combined effects. As considered in [42] we first assume that external pressure modifies the crystal field splittings of the 3*d* manifold, and we look for an electronic instability of the hexagonal phase as a function of applied pressure. This assumption is known to be plausible and it

has already been successfully used by other groups to study the effect of pressure and/or lattice strain on the orbital-selective electronic reconstruction of correlated electron systems [43, 44]. However, it is recognized that under external perturbations like pressure and strain, the hopping elements and the crystal field splittings are renormalized in non-trivial ways. In practice it is difficult to separate the effects of the hopping from those induced by crystal field splittings, especially if the correlated electronic structure under pressure is not known *a priori*. With this caveats in mind, we study the effect of the orbital splittings on the correlated many-body states of *h*-FeS. Differently to [41] we do not change the LDA DOS to derive pressure induced phase transitions. Instead, we search for the instability of the low-pressure phase towards a distinct phase as pressure is varied. This approximation is justified, because we do not expect much correspondence between changes in the one-band quantities with those affected in non-trivial ways by dynamical electronic correlations. Actually, compared to our LDA calculation the LDA+DMFT results reveal changes in the ground state orbitals. While in LDA the xy, x^2-y^2 are the ground state orbitals, at $U = 5.0$ eV the lowest orbital is the $3z^2-r^2$ followed, respectively, by the doubly degenerated xz,yz and the xy, x^2-y^2 channels[5].

Under AP conditions, iron in FeS is divalent with HS ($S = 2$) configuration and goes towards to a LS ($S = 0$) state with increasing pressure [14]. Therefore, we consider the orbital-dependent on-site energy term [45–47], $H_\Delta = \sum_{i,a,\sigma} \Delta_a n_{i,a,\sigma}$ in our Hamiltonian $H = H_0 + H_{\rm int}$ (equations (1) and (2)) for *h*-FeS. Within LDA+DMFT we now vary Δ_a in small steps, assuming $\Delta_{xz,yz,3z^2-r^2} = -\Delta$ and $\Delta_{xy,x^2-y^2} = \Delta$ to mimic the spin-state transition [48] in FeS, and the underlying electronic reconstruction with pressure. Here, Δ_a acts like an external field in the orbital sector (orbital fields), sensitively controlling the occupations of each orbital (see figure 7) in much the same way as the magnetization of a paramagnet as function of an external magnetic field. However, in order to draw a qualitative interpretation of H_Δ in our total model Hamiltonian $\bar{H} = H + H_\Delta$ and its relation to pressure-induced electronic reconstruction in FeS, we recall that the pressure derivative of crystal-field splitting is given by $\mathrm{d}\Delta/\mathrm{d}P = \xi\Delta/K$, where K is the bulk modulus and ξ is a constant value [49]. This in turn suggests that in the pressure range of interest in this work $h-$ FeS could be in a linear regime as observed in other materials under external pressure conditions [50]. Thus, to show how changes in the correlated electronic structure and *dc* transport responses of pressurized *h*-FeS might be explained by a modification of Δ is our focus below.

We now study the orbital-selective metallic state obtained as an instability of the correlated Mott insulator derived above for $U = 5.0$ eV. In other works, the transition towards a paramagnetic metallic and insulating states [25] in pressurized FeS is derived not by changing the LDA DOS with pressure as in [9], for example, but by searching for an instability of the paramagnetic insulating state under pressure. In reality, as proposed earlier to describe the insulator-metal transition of V_2O_3 under external pressure [42], one has to study the transition to the insulating-metallic-insulating phases of FeS without leaving the strongly correlated picture, and derive the transitions by searching for the correlated solution of the DMFT equations under pressure. To justify our approach, we specify the problem associated with the approach used, for example, by Ushakov *et al* [9]. First, it is theoretically inconsistent to derive a phase transition between two strongly correlated electronic phases by using corresponding LDA band structures to separately derive the two phases. This is because using changes in bare LDA parameters to study correlated phases is problematic, since these parameters have no clear meaning in a multi-orbital correlated electron picture. One must use the renormalized values of these parameters instead, and these are generically modified in unknown ways by strong MO correlation effects. These changes in bare LDA parameters, and the modification of the response of correlated electrons to these changes, must be self-consistently derived within the LDA+DMFT procedure. Clearly, this route has not been used in recent band structure approaches to correlated quantum materials under external pressure and ours is the first in this direction for *h*-FeS. Thus, as in [42] we adopt the following strategy. We hypothesise that external pressure modifies the crystal-field splittings or the on-site energy levels, which in turn self-consistently control the orbital occupancies of the different orbital sectors. To our knowledge, our approach is not totally new: Mott and co-workers proposed such ideas in the 1970s [51]. Tanaka made a similar hypothesis in a cluster model approach for V_2O_3 [43] and Savrasov *et al* [52] have employed similar ideology to study the volume collapse across the $\alpha-\delta$ transition in Plutonium.

In a correlated electron system, small changes in the local energy splittings lead to large dynamical SWT typically over a scale of few electron-Volts [45]. As seen in figure 5, at values of Δ below 1.2 eV we observe systematic changes, albeit with different SWT, in the orbital-resolved spectral functions with pressure. In this parameter range the xz,yz orbitals remain Mott localized while asymmetric quasiparticle (Kondo-like) resonance are formed in the xy, x^2-y^2 orbitals at low-binding energies, and they move towards $E_{\rm F}$ with increasing Δ. Given our choice for Δ_a the valence band states of the $xz, yz, 3z^2-r^2$ orbitals are lowered in energy while the xy, x^2-y^2 orbitals move to higher frequencies. This in turn enhances the orbital splitting of *h*-FeS found in LDA+DMFT for $\Delta = 0$ due to intrinsic dynamical SWT across the spin-state transition in FeS. Interesting in figure 5 are also the changes in the position of the lower Hubbard bands of the $3z^2-r^2$ orbital, which are transferred to high binding energies with increasing Δ. Taken together, up to $\Delta = 1.2$ eV *h*-FeS is in a two-fluid regime [42], characterized by the coexistence

[5] At $U = 5.0$ eV the gravity centers of the different LDA+DMFT bands are $\epsilon_{xy,x^2-y^2} = -1.348$ eV, $\epsilon_{xz,yz} = -1.618$ eV, $\epsilon_{3z^2-r^2} = -1.789$ eV, meaning that $3z^2-r^2$ is the ground state orbital of *h*-FeS at ambient pressure condictions.

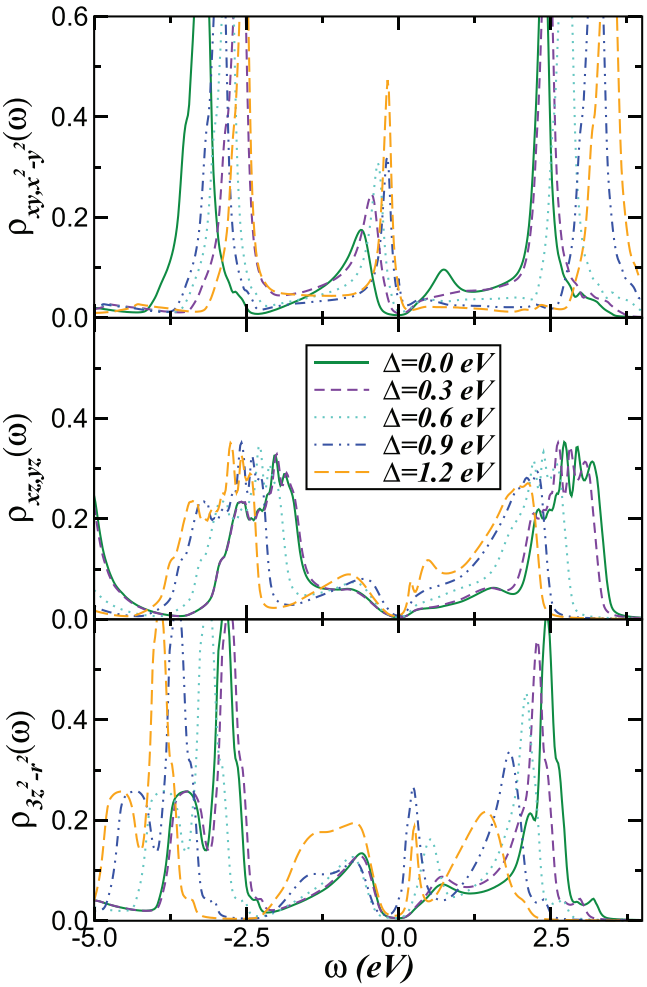

Figure 5. Evolution of the LDA+DMFT ($U = 5$ eV, $J_H = 0.7$ eV) orbital-resolved spectral functions of hexagonal FeS for different values of the crystal-field splitting Δ. Notice the modification of the LDA+DMFT density-of-states due to large-scale dynamical spectral weight transfer with increasing Δ. While the $xz, yz, 3z^2 - r^2$ orbitals remain localized, an asymmetric quasiparticle resonance sets in within $xy, x^2 - y^2$ channels due to pressure-induced selective-orbital reconstruction.

of pseudogaped and Mott-localized electronic states at low energies. This behavior is consistent with that found for pressurized FeO with rocksalt-type structure [11], and it is characteristic of a bad-metal system.

Let us now describe the band structure across the insulator-metal-insulator [25] transition point of pressurized FeS. As seen in figure 6, the $xy, x^2 - y^2$ orbitals are the most affected by pressure at low energies. In these orbitals, the Kondo quasiparticle resonances shrink dramatically and intersect the Fermi level with increasing Δ. Thus, the transition we have found is characterized by the presence of low energy quasiparticle dispersions which are piked at E_F for $\Delta_c = 1.4$ eV. Similar low-energy orbital reorganization across the pressure-driven insulator-to-metal transition was obtained for transition-metal mono-oxides [41, 53], hematite [54] as well as in $YTiO_3$ [45], suggesting a common (albeit orbital dependent) underlying scenario for pressurized transition-metal compounds. Here, we emphasize that coexistence of insulating $(3z^2 - r^2)$, pseudogaped (xz,yz) and metallic $(xy, x^2 - y^2)$ states at $\Delta_c = 1.4$ eV is the key mechanistic step, which allows to understand the strange metallic behavior observed in pressurized FeS [25]. Hence, it would be interesting to see whether this selective orbital mechanism with a sharp Kondo-quasiparticle resonances near E_F would be observable in angle-resolved PES (ARPES) spectroscopy of pressurized FeS.

Finally, in figure 7 we display the averaged occupation numbers $\langle n_{\sigma,a} \rangle$, computed using the LDA+DMFT orbital resolved spectral functions of FeS. As in [41] we observe kinks for $\Delta \geqslant 1.1$ eV. This response is characteristic of strongly correlated materials, where the orbital occupation is linked to dynamical orbital fluctuations in the reconstructed electronic state. The role of Δ is apparent in our results of figure 7, acting exactly like an orbital field. Notably, orbital polarization is enhanced under the application of pressure, driving changes in orbital occupations. However, in spite of previos experimental evidences towards to a HS-to-LS state transition [7, 14] our results in figure 7 suggest a gradual HS to intermediate spin (IS) state transition which is consistent with the spin-crossover scenario of iron in the ferropericlase solid solution at Earth's mid-lower mantle condictions [55]. This because full orbital polarization characteristic of a LS state [56] will only be achieved using higher values of Δ than those considered in this work. Thus, our results suggest that near the hexagonal-to-monoclinic structural transition FeS should be closer to an IS state.

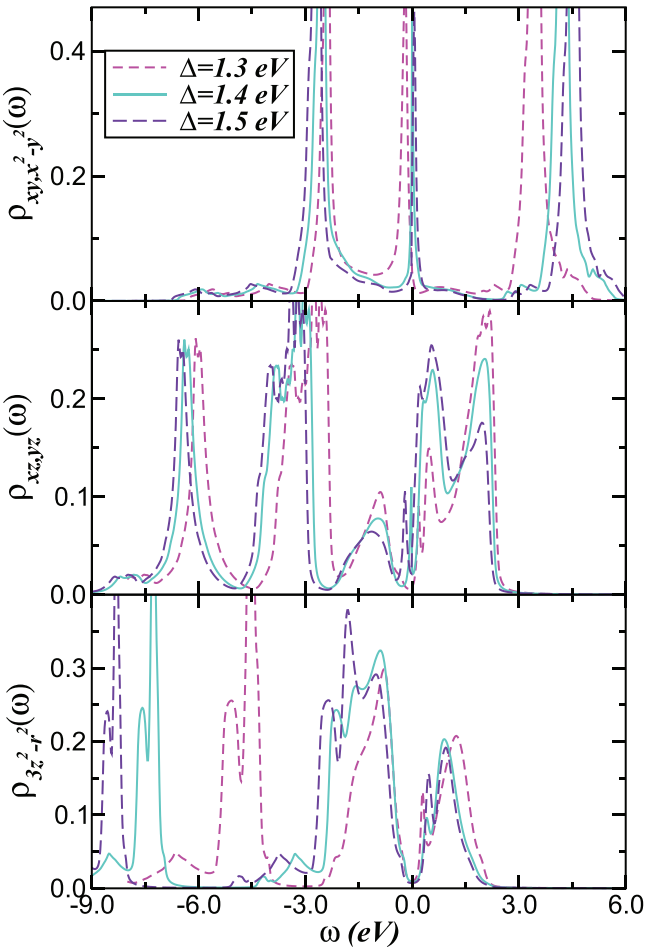

Figure 6. LDA+DMFT orbital-resolved DOS of hexagonal FeS at the border of the pressure-induced insulator-to-metal transition. Notice the modification of the LDA+DMFT spectral functions due to large-scale dynamical spectral weight transfer with increasing Δ towards to its critical value. While the xy, x^2-y^2 orbitals show a quasiparticle resonance at the Fermi energy, the $3z^2-r^2$ orbital remain Mott localized.

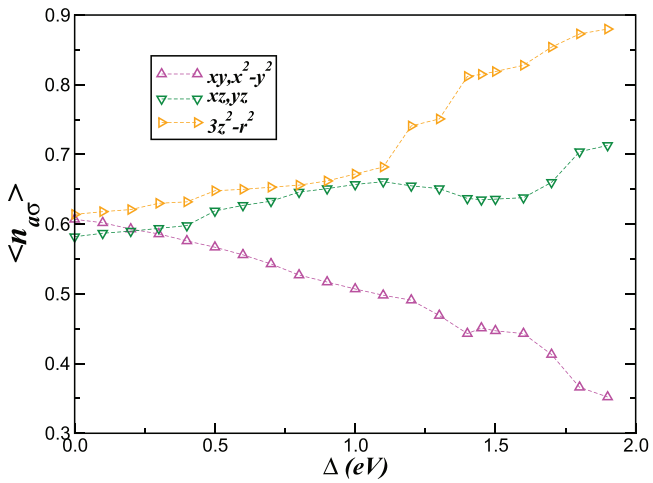

Figure 7. Fe-3d occupancies as function of Δ obtained within LDA+DMFT calculations for $U = 5.0$ eV and $J_H = 0.7$ eV. Notice the changes in $\langle n_{a,\sigma}\rangle$ at $\Delta \geqslant 1.1$ eV.

2.3. Transport properties of hexagonal FeS

In an earlier work, we have shown that the MO correlated nature of h-FeSe system [31] can be semiquantitatively understood using LDA+DMFT with sizable d-band correlations. Here, we extend this aspect to characterize the electrical properties of stoichiometric h-FeS under pressure. Specifically, we study the T-dependence of the dc resistivity and correlate it with the orbital-reconstruction scenario derived above. Given the correlated spectral functions

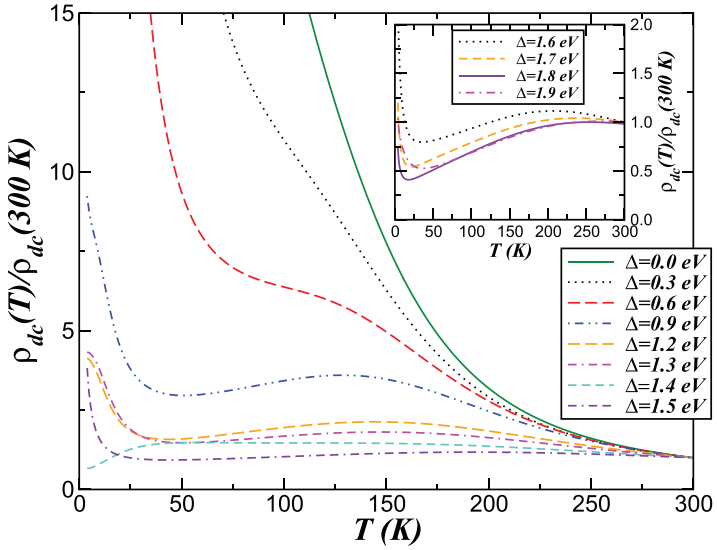

Figure 8. T-dependence of electrical resistivities for Mott-insulating ($\Delta = 0.0$ eV) and pressurized ($\Delta \geqslant 0.3$ eV) FeS , showing qualitative good accord with transport data [14, 25]. Particularly interesting is the insulating-metallic-insulating behavior for 1.3 eV$\leqslant \Delta \leqslant$1.5 eV consistent with data of [25]. Inset display resistivity curves at higher Δ, showing small resistivity upturns at low temperatures. This behavior is characteristic of bad-insulators.

$A_a(\mathbf{k},\omega) = -\frac{1}{\pi}\mathrm{Im}\ G_a(\mathbf{k},\omega)$ (with $a = xy, xz, yz, x^2-y^2, 3z^2-r^2$) the (static) dc conductivity $[\sigma_{dc}(T)]$, computed within the Kubo formalism, [57] can be expressed as $\sigma_{dc}(T) = \frac{\pi}{T}\sum_a \int \mathrm{d}\epsilon\, \rho_a^{(0)}(\epsilon) \int \mathrm{d}\omega A_a^2(\epsilon,\omega) f(\omega)[1-f(\omega)]$. In this expression, $\rho_a^{(0)}(\epsilon)$ is the LDA DOS of the a-bands (figure 3) and $f(\omega)$ is the Fermi function.

In figure 8 we display the T-dependence of electrical resistivity $[\rho_{dc}(T) \equiv 1/\sigma_{dc}(T])$ with increasing Δ, computed using the LDA+DMFT orbital resolved spectral functions for $U = 5.0$ eV in $\sigma_{dc}(T)$. Various interesting features immediately stand out. First, $\rho_{dc}(T \to 0)$ is large with clear insulating like behavior at $\Delta = 0$, in accordance with the Mott insulating description above. This Mott-localized behavior is smoothly suppressed with increasing Δ and disappears in the orbital-selective metallic phase at $\Delta_c = 1.4$ eV, see figure 6. Noteworthy, above this critical value the resistivity curves show a small insulating upturn below 20 K. Interestingly, the detailed T-dependence in figure 8 resembles the one seen in experiments [14, 25], showing insulator-metal-insulator transitions [25] with increasing pressure from AP to 8.0 GPa.

To rationalize the overall bad-insulating behavior, which is characterized by a small resistivity upturn at low temperatures in pressurized FeS, it is worth noting that localization of the $d_{3z^2-r^2}$ states at $\Delta \geqslant 1.5$ eV in figure 6 implies that this orbital act like an intrinsic source of electronic disorder in the system. This implies that an intrinsic disorder potential, arising from orbital-selective physics, exists in FeS at pressures close to 8.0 GPa. Remarkably, such behavior results from strong scattering between effectively Mott-localized and itinerant components of the full DMFT propagators. This is intimately linked to orbital-selective Mott-like physics within DMFT [58]. We note that such orbital-selective physics has also been proposed earlier for h-FeSe system [31] as well as on phenomenological grounds for iron-pnictides superconductors [59]. The qualitative agreement between our resistivity results close to Δ_c and that seen in experiments [25], suggests appreciable $3z^2-r^2$-orbital reconstruction at high-binding energies which might belinked with the hexagonal-monoclinic structural phase transition in FeS. Future theoretical and experimental work to corroborate our prediction are called for.

3. Conclusion

We have used LDA+DMFT on a five-band Hubbard model to derive a correlation- and pressure-induced orbital reconstruction in hexagonal iron sulfide. We have analyzed its Mott-insulating nature, baring it as an effect of multi-orbital dynamical correlations. Upon consideration of pressure effects we observe continuos changes in dynamical spectral weight transfer at high- and low-energies. Particularly interesting is the emergence of narrow Kondo quasiparticles in the xy, x^2-y^2 orbitals with increasing pressure, which is our mechanism for insulator-metal-insulator instabilities seen in pressurized FeS. According to our results, the electronic reorganization with pressure is manifested in structural changes at a critical energy splitting which destabilises the hexagonal crystal structure under pressure. The interplay between Mottness-induced selective electronic localization and bad-itinerancy in hexagonal FeS suggests a promising and practical route to access electronic, magnetic and transport properties at planetary core conditions [1, 60], but this problem of fundamental and practical importance remains to be seen in future.

Acknowledgments

LC's work is supported by CNPq (Proc. No. 307487/2014-8). Acknowledgment (LC) is also made to Theoretical Chemistry department at Technical University Dresden for hospitality. SL thanks the DFG for support under the priority project SPP 1415 and for a personal Heisenberg grant. SL acknowledges support from the UK Research Council under Project No. EP/M50631X/1. ZIH Dresden and ARCCA Cardiff (SL) are acknowledged for the generous allocation of computational resources.

References

[1] Fei Y *et al* 1995 *Science* **268** 1892
[2] Ono S *et al* 2008 *Earth Planet. Sci. Lett.* **272** 481
[3] Urakawa S *et al* 2004 *Phys. Earth Planet. Inter.* **143–4** 469
[4] Duffy T S 2005 *Rep. Prof. Phys.* **68** 1811
[5] Kusaba K, Syono Y, Kikegawa T and Shimomura O 1998 *J. Phys. Chem. Solids* **59** 945
[6] Shimada K *et al* 1998 *Phys. Rev.* B **57** 8845
[7] Rueff J-P *et al* 1999 *Phys. Rev. Lett.* **82** 3284
[8] Guénon S *et al* 2015 arXiv:1509.04452
[9] Ushakov A V *et al* 2016 arXiv:1608.02360
[10] Ovchinnikov S G *et al* 2012 *JETP Lett.* **96** 129
[11] Ohta K *et al* 2012 *Phys. Rev. Lett.* **108** 026403
[12] Liao F *et al* 2013 *Appl. Surf. Sci.* **283** 888
[13] Rui X, Tan H and Yan Q 2014 *Nanoscale* **6** 9889
[14] Takele S and Hearne G R 1999 *Phys. Rev.* B **60** 4401
[15] Li Y, van Santen R A and Weber Th 2008 *J. Solid State Chem.* **181** 3151
[16] Pachmayr U, Fehn N and Johrendt D 2016 *Chem. Commun.* **52** 194
Borg C K H *et al* 2016 *Phys. Rev.* B **93** 094522
[17] Tremel W, Hoffmann R and Silvestre J 1986 *J. Am. Chem. Soc.* **108** 5174
[18] Kobayashi H *et al* 2005 *Phys. Rev.* B **71** 014110
[19] Denholme S J *et al* 2014 *Mater. Chem. Phys.* **147** 50
[20] Shu-Lin Z, Hui-Xian W and Cheng D 2014 *Chin. Phys.* B **23** 087203
[21] Denholme S J *et al* 2014 *Sci. Technol. Adv. Mater.* **15** 055007
[22] Bertaut E F, Burlet P and Chappert J 1965 *Solid State Commun.* **3** 335
Mullet M *et al* 2002 *Geochim. Cosmochim. Acta* **66** 829
[23] Deguchi K, Takano Y and Mizuguchi Y 2012 *Sci. Technol. Adv. Mater.* **13** 054303
[24] Chen L, Matsunami M, Nanba T and Kobayashi H 2006 *Physica* B **378–80** 1116
[25] Kobayashi H *et al* 2001 *Phys. Rev.* B **63** 115203
[26] Horwood J L, Townsend M G and Webster A H 1976 *J. Solid State Chem.* **17** 35
[27] Imada M, Fujimori A and Tokura Y 1998 *Rev. Mod. Phys.* **70** 1039
[28] Craco L and Leoni S 2014 *Mater. Res. Express* **1** 036001
[29] Subedi A, Zhang L, Singh D J and Du M H 2008 *Phys. Rev.* B **78** 134514
[30] Kotliar G *et al* 2006 *Rev. Mod. Phys.* **78** 865
[31] Craco L and Leoni S 2010 *Europhys. Lett.* **92** 67003
[32] Andersen O K 1975 *Phys. Rev.* B **12** 3060
[33] Chadov S *et al* 2010 *Nat. Mater.* **9** 541
Borisenko S V *et al* 2016 *Nat. Phys.* **12** 311
[34] Boness D A and Brown J M 1990 *J. Geophys. Res.: Solid Earth* **95** 21721
[35] Antonov V N *et al* 2009 *Phys. Status Solidi* B **246** 411
[36] Craco L and Faria J L B 2016 *J. Appl. Phys.* **119** 085107
[37] Nelmes R J *et al* 1999 *Phys. Rev.* B **59** 569
[38] Craco L 2008 *Phys. Rev.* B **77** 125122
[39] Kajueter H and Kotliar G 1996 *Phys. Rev. Lett.* **77** 131
[40] Georges A, Kotliar G, Krauth W and Rozenberg M J 1996 *Rev. Mod. Phys.* **68** 13
[41] Shorikov A O *et al* 2010 *Phys. Rev.* B **82** 195101
[42] Laad M S, Craco L and Müller-Hartmann E 2006 *Phys. Rev.* B **73** 045109
[43] Tanaka A 2002 *J. Phys. Soc. Japan* **71** 1091
[44] Poteryaev A I, Ferrero M, Georges A and Parcollet O 2008 *Phys. Rev.* B **78** 045115
Mukherjee S *et al* 2016 *Phys. Rev.* B **93** 241110
[45] Craco L, Laad M S, Leoni S and Rosner H 2008 *Phys. Rev.* B **77** 075108
[46] de' Medici L *et al* 2009 *Phys. Rev. Lett.* **102** 126401
Kita T, Ohashi T and Kawakami N 2011 *Phys. Rev.* B **84** 195130
Huang L, Du L and Dai X 2012 *Phys. Rev.* B **86** 035150
Jakobi E, Blümer N and van Dongen P 2013 *Phys. Rev.* B **87** 205135
[47] Schüler M *et al* 2016 *Phys. Rev.* B **93** 195115
[48] Craco L and Müller-Hartmann E 2008 *Phys. Rev.* B **77** 045130
[49] Sturhahn W, Jackson J M and Lin J-F 2005 *Geophys. Res. Lett.* **32** L12307
[50] Hernández D *et al* 1999 *Physica* B **265** 186
Manjón F J *et al* 2004 *Phys. Rev.* B **69** 165121
[51] Mott N F 1974 *Metal-Insulator Transitions* (London: Taylor and Francis)
[52] Savrasov S Y, Kotliar G and Abrahams E 2001 *Nature* **410** 793

[53] Huang L, Wang Y and Dai X 2012 *Phys. Rev.* B **85** 245110
Kunes J *et al* 2008 *Nat. Mater.* **7** 198
[54] Kunes J *et al* 2009 *Phys. Rev. Lett.* **102** 146402
[55] Lin J F *et al* 2007 *Science* **317** 1740
[56] Leonov I 2015 *Phys. Rev.* B **92** 085142
[57] Haule K and Kotliar G 2009 *New. J. Phys.* **11** 025021
[58] Biermann S, de' Medici L and Georges A 2005 *Phys. Rev. Lett.* **95** 206401
[59] Hackl A and Vojta M 2009 *New J. Phys.* **11** 055064
[60] Gubbins D, Sreenivasan B, Mound J and Rost S 2011 *Nature* **473** 361